FIRST RESULTS FROM THE XMM-NEWTON OBSERVATION IN THE GROTH-WESTPHAL SURVEY STRIP REGION

Takamitsu Miyaji, Richard E. Griffiths

Department of Physics, Carnegie Mellon University

5000 Forbes Av., Pittsburgh PA 15213, USA

We present the first results of the XMM-Newton observation on the Groth-Westphal Strip Field. The scheduled exposure time was 70 [ks]. We first analyzed ~ 50 [ks] of calibrated and cleaned EPIC-PN data, which were the only ones we could successfully process with an early version of the SAS software applicable to these observations. A total of ~ 110 sources have been detected in the central 10 arcmin of the PN field of view (FOV). A cross-correlation with the Hubble Space Telescope (HST) Medium Deep Survey (MDS) database shows a range of morphological properties of host galaxies of the X-ray source. Spectra of hard X-ray sources in our data indeed show absorption in the range $N_{\rm H} \sim 10^{22} - 10^{23} [{\rm cm}^{-2}]$ at $z \sim 1$.

1 Introduction

The Groth-Strip field is one of the best-studied fields in extragalactic astronomy. The Groth-Strip Campaign started from 28 contiguous medium-deep HST Wide-Field Planetary Camera 2 (WFPC2) images by E. Groth[3], followed by numerous follow-up projects over the entire electromagnetic spectrum.

In this field, we are investigating the population of X-ray sources using our XMM-Newton guaranteed time observation (PI=Griffiths), with an emphasis on morphological properties of the X-ray sources, taking advantage of the sharp WFPC2 images and the HST MDS database[5] with extensive disk-bulge morphological characterizations.

2 The Data

The observations were made during revolutions 111-114 (July 2000). The period of low particle background is concentrated in revolution 113. We were able to generate a cleaned and calibrated dataset for only EPIC-PN from the available software at the time of this preliminary analysis. With the most recent version of SAS (5.1 beta) at the time of writing this paper, we have been able to generate calibrated datasets for the MOS detectors also and we are starting the analysis of the combined PN and MOS dataset.

Three broad-line AGNs in the CFRS v1.0[4] catalog and three AGN candidates in Beck-Winschatz & Anderson [1] (BWA) have X-ray counterparts in our EPIC-PN image. Positions of the X-ray sources have been determined by single or multiple-source elliptical gaussian fits. The X-ray data have been aligned by matching these positions with known optical positions of these AGNs. The positional errors of the fits (90% along each axis) were $\lesssim 1''$. The residuals of the alignment were typically $\lesssim 1''$ and the largest residual was $2''$. Fig. 1 shows the PN image (smoothed with a $\sigma = 6''$ gaussian) with a number of overlays as indicated in the caption.
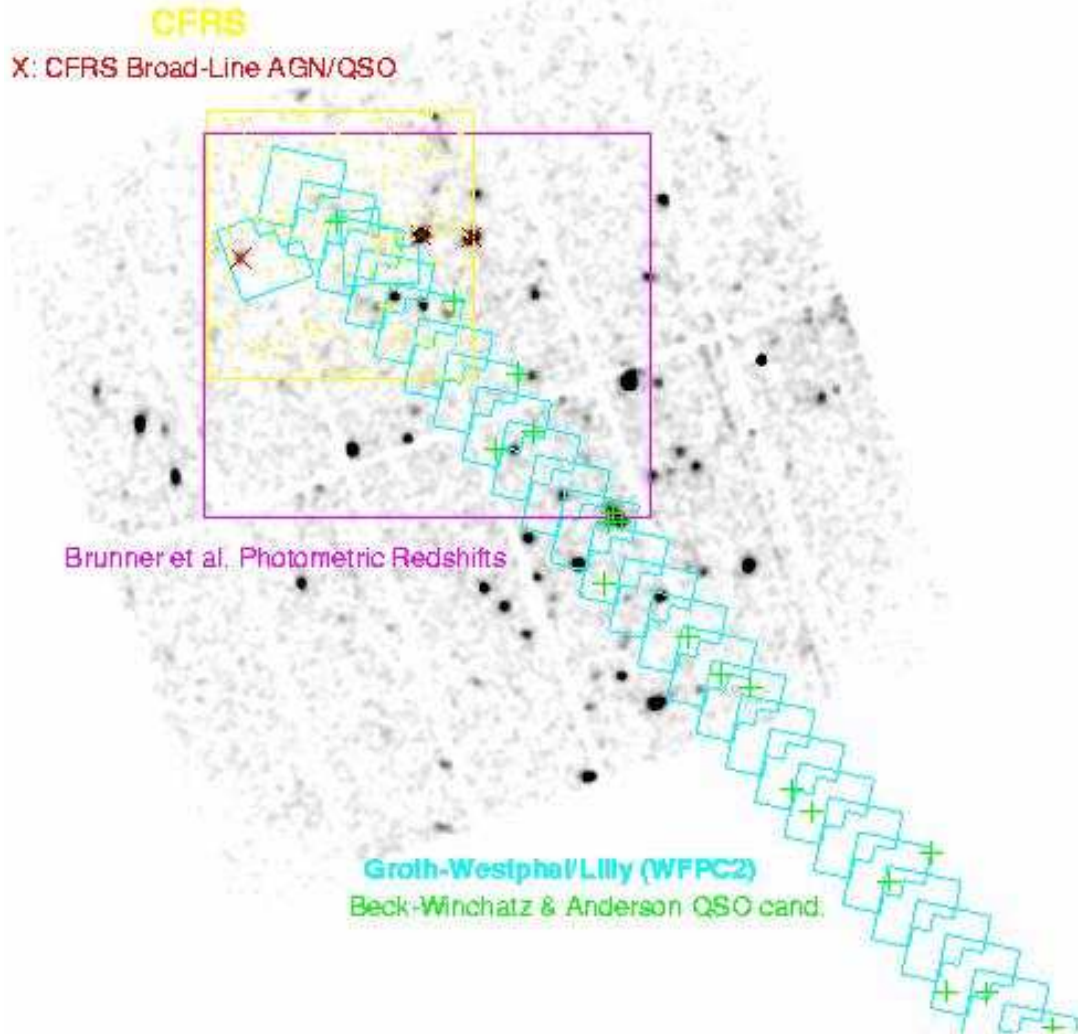
Figure 1: The XMM-Newton EPIC-PN image (underlying grayscale) of the Groth-Strip, smoothed with a $\sigma = 6''$ gaussian, is shown with WFPC2 FOVs (cyan), the CFRS[4] FOV and galaxies with redshifts (yellow), broad-line AGNs in the CFRS (red cross) and the region with the photometric redshift catalog by Brunner et al.[2] (magenta). The XMM-Newton PN FOV is $27' \times 27'$.

Table 1: Groth-Westphal Field EPIC-PN 50 ks

Energy [keV]	N_det $(N_\mathrm{hot})^{a)}$	$S_\mathrm{x}^\mathrm{min}$ $^{b)}$ [$\mathrm{erg\,s^{-1}\,cm^{-2}}$]
0.5-7.0	113 $(\gtrsim 6)$	$2 \cdot 10^{-15}$
0.5-2.0	92 $(\gtrsim 9)$	$7 \cdot 10^{-16}$
2.0-4.5	39 $(\gtrsim 0)$	$2 \cdot 10^{-15}$
4.5-10	18 $(\gtrsim 0)$	$8 \cdot 10^{-15}$

a) Number of sources over 324 arcmin^2. a) Sensitivity varies over the FOV and the approximate detection limits show here are estimated near the optical axis.

Table 2: MDS Morphologies of X-ray sources

Stellar	Disk+Bulge	Pure Bulge	Galaxy$^{a)}$	No MDS entry
3	2	3	2	2

a) An extended component has been resolved but the galaxy is too faint for a disk/bulge discrimination.

3 Preliminary Source Detection

Preliminary source detection has been made on the 50 ks of EPIC-PN data using the automated source-detection task *edetectproc* in SAS 5.0 with a likelihood threshold of $-\ln P = 15$, where P is the probability that the source does not exist (approximately corresponding to a 5σ detection). The numbers of sources in different bands (N_det) and the approximate detection thresholds ($S_\mathrm{x}^\mathrm{min}$) are shown in Table 1. There are unremoved hot pixels and columns in our current data and the source detection procedure also recognized peaks of these features as real sources. Table 1 shows the number of the sources which apparently come from the hot columns also (N_hot). Note that we are likely to miss the recognition of spurious sources which are more subtle. Exclusion of all spurious sources will be possible in the future by matching up the PN and MOS source lists. An approximate detection limit for each band is shown. For the count rate-to flux conversion, the PIMMS software was used with a $\Gamma = 1.4$ power-law with Galactic absorption ($N_\mathrm{H} = 1 \cdot 10^{20} [\mathrm{cm^{-2}}]$).

4 X-ray sources in the HST WFPC2 Fields

In the strip of the HST WFPC2 fields, BWA[1] selected 20 QSO/AGN candidates based on the existence of point-like cores and UV-excess down to ($B \lesssim 24.5$), among which 11 objects are within our EPIC-PN FOV. A quick match with our PN data immediately revealed the difficulty of selecting AGNs from numerous objects in the optical/UV data. Out of the 11 AGN candidates and 12 X-ray sources in the overlapping area, only 3 sources match. While there are possibilities that some of the BWA AGN candidates are actually X-ray weak AGNs (e.g. BAL QSOs), it is also possible that their compact-core UV-excess criteria selects galaxies with circum-nuclear starbursts as well.

The existence of HST WFPC2 images in this field immediately enables us to investigate the morphological properties of the X-ray sources. In particular, it allowed immediate comparison with the MDS[5] database, which contains the results of extensive disk-bulge separations for galaxies. Table 2 shows the number of X-ray sources in each morphological category in the MDS database (for the F814W filter, where the stellar population in host galaxies is more enhanced when compared with the star-like AGN). The WFPC2 images (from the MDS database[5]) for four of the X-ray sources are shown in Fig. 2 with known properties in the caption.
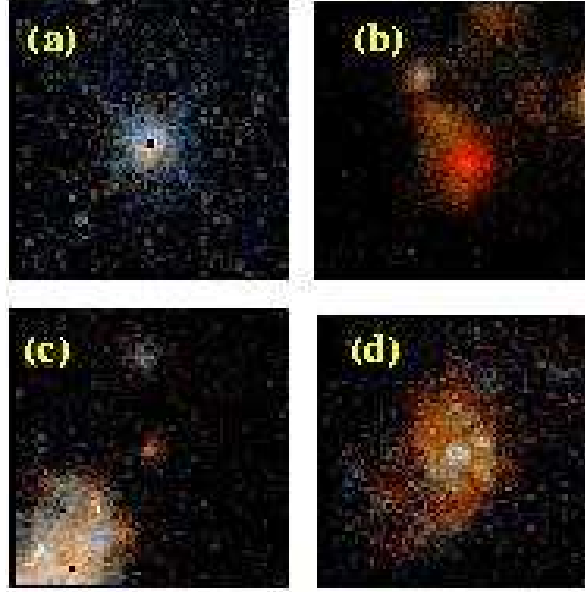
Figure 2: The WFPC2 morphologies of selected X-ray sources in the Groth-Strip Filed are shown. The images have 64× 64 pixels with $0.1''$/pixel(a)(c)(d) or $0.046''$/pixel (b). (a): a broad-line QSO with z=1.6, stellar image (b): Seyfert 2, z=1.15, the X-ray spectrum shows absorption and the WFPC2 image can be fitted with a pure-bulge. Possibly interacting. (c) the X-ray source is a very faint galaxy (not a point source) with F606W= 26.2 [mag]. (d) $z \sim 0.8$ Seyfert 1. Disk+Bulge WFPC2 image.

5   Spectra of Selected Sources

XMM-Newton enabled us to investigate spectra of faint $(S_{\mathrm{x}} \lesssim 10^{-14} \ [\mathrm{erg\,s^{-1}\,cm^{-2}}])$ sources. With *ASCA*, *Beppo-SAX* and *Chandra* data, it was not still clear whether these faint "hard" sources have actually absorbed spectra, intrinsically hard, and/or reflection-dominated. Fig. 3 shows two examples of absorbed spectra found in the XMM-Newton data. These clearly indicate absorbed spectra.
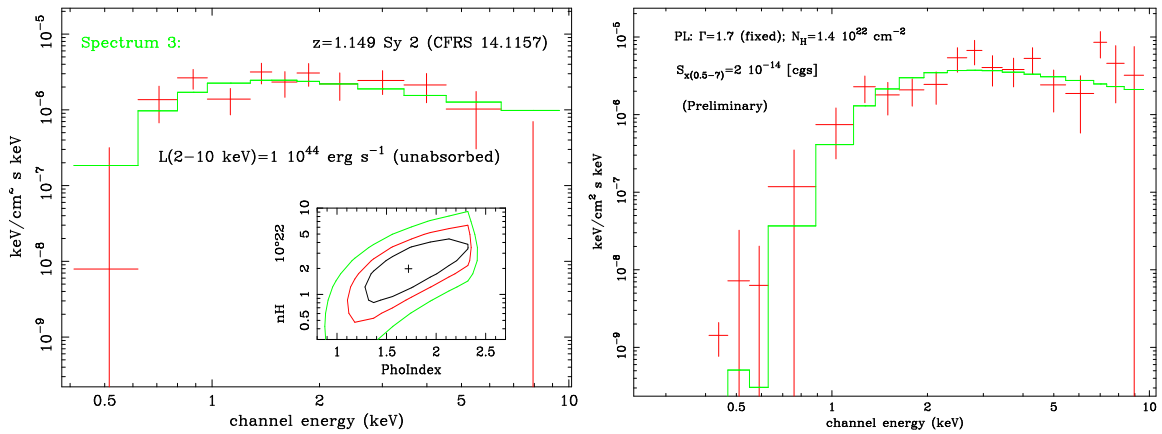
6   Summary

Figure 3: EPIC-PN unfolded Spectra of two of hard X-ray sources on the Groth-Westphal Strip region are shown. Note that the absolute flux calibration of the response matrix used in these fits was still highly uncertain.

1. First results from the XMM-Newton observations on the Groth-Westphal Strip Filed have been presented. About 50 [ks] of EPIC-PN data have been analyzed thus far.

2. With a preliminary source detection, we obtained $\sim$ 110 X-ray sources to a limiting flux of 2×10^{-15} [erg s^{-1} cm^{-2}] (0.5-2 [keV]) in the central 10 arcmin-radius region, a small fraction of which are still unremoved hot pixels and columns.

3. We have investigated the morphological properties of the optical counterparts of the 12 X-ray sources which are within the HST WFPC2 FOVs. The X-ray sources show a variety of morphological properties.

4. The large effective area of XMM-Newton enabled us to obtain good spectroscopic data on faint hard X-ray sources. They indeed show evidence that they are absorbed AGNs.

Acknowledgments

References

1. Beck-Winchatz B. & Anderson F. 1999, AJ 117, 2582
2. Brunner, R.J. et al. 2000, ApJ 541, 527
3. Groth E. et al. 1994, BAAS 185, 5309
4. Lilly, S.J et al. 1995 ApJ 455, 75
   (`http://www.astro.utoronto.ca/lilly/CFRS`)
5. Ratnatunga, K. U., Griffiths, R. E., & Ostrander, E. J. 1999, AJ 118, 86
   (`http://archive.stsci.edu/mds`)